10-2016

pHLIP Peptide Interaction with a Membrane Monitored by SAXS

Theyencheri Narayanan

Dhammika Weerakkody
University of Rhode Island

Alexander G Karabadzhak
University of Rhode Island

Michael Anderson

Oleg A. Andreev
University of Rhode Island, andreev@uri.edu

See next page for additional authors

Citation/Publisher Attribution

Narayanan, T., Weerakkody, D., Karabadzhak, A. G., Anderson, M., Andreev, O. A., & Reshetnya, Y. K. pHLIP Peptide Interaction with a Membrane Monitored by SAXS. J*J. Phys. Chem. B* 2016 *120*(44), 11484-11491. doi: 10.1021/acs.jpcb.6b06643
Available at: http://doi.org/10.1021/acs.jpcb.6b06643

pHLIP® Peptide Interaction with Phospholipid Membrane Monitored by SAXS

Theyencheri Narayanan[1,], Dhammika Weerakkody[2], Alexander G. Karabadzhak[2,†], Michael Anderson[2], Oleg A. Andreev[2], Yana K. Reshetnyak[2,*]*

[1]ESRF – The European Synchrotron, 38043 Grenoble, France

[2]Department of Physics, University of Rhode Island, Kingston, RI 02881

ABSTRACT

The pH (Low) Insertion Peptides (pHLIP® peptides) find application in studies of membrane-associated folding, since spontaneous insertion of these peptides is conveniently triggered by varying pH. Here we employed small angle X-ray scattering (SAXS) to investigate WT pHLIP® peptide oligomeric state in solution at high concentrations and monitor changes in liposome structure upon peptide insertion into the bilayer. We established that even at high concentrations (up to 300 μM) WT pHLIP® peptide at pH 8.0 does not form oligomers higher than tetramers (which exhibit concentration-dependent transfer to monomeric state as it was shown previously). This finding has significance for medical applications, when high concentration of the peptide is injected into blood and diluted in blood circulation. The interaction of WT pHLIP® peptide with liposomes does not alter the unilamellar vesicle structure upon peptide adsorption by lipid bilayer at high pH or upon insertion across the bilayer at low pH. At the same time, SAXS data clearly reflect the insertion of the peptide into the membrane at low pH, which opens the possibility to investigate kinetic process of a polypeptide insertion and exit from the membrane in real time by time-resolved SAXS.

Introduction

Folding and insertion into membrane of constitutive membrane proteins is facilitated by complex molecular machines *in vivo,* including the translocon that places most transmembrane (TM) helices across the bilayer (1-3). While they are assisted in their pathways by the Get proteins(4), non-constitutive membrane proteins (such as tail-anchored proteins) can spontaneously insert and fold themselves across the lipid bilayer of a membrane. They may do so when released by the Get complex *in vivo* (5, 6). The molecular mechanisms of spontaneous polypeptide folding/insertion and exit/unfolding are of interest in several contexts including the action of antimicrobial peptides, the folding and degradation of membrane proteins, and biotechnological/medical applications based on these processes.

Stability and folding of all membrane proteins, irrespective of mechanism of their insertion into membrane, are governed by the formation of polypeptide secondary structures in the lipid bilayer environment, driven by the hydrophobic interactions and by hydrogen bonding. A convenient experimental approach is to trigger a coil-helix transition and peptide insertion into a bilayer by a pH jump. The protonation enhances the hydophobicity of the peptide and, therefore, its affinity to the nonpolar environment of a membrane. One such case of a synthetic peptide with pH-dependent membrane-insertion properties has been investigated by White and Ladokhin (7). Another example is the pH Low Insertion Peptide (pHLIP® peptides) family, which is the subject of this study.

The wild type (WT) pHLIP® peptide was derived from the C-helix of bacteriorhodopsin (8, 9). Later, many different pHLIP® variants were introduced (10-15). All peptides share the same property: pH-dependent insertion into lipid bilayer of membrane, which is accompanied by a coil-helix transition and formation of a transmembrane (TM) helix. Importantly, the main principle of membrane-associated folding was employed to introduce a novel class of rationally designed pHLIP® delivery agents. The pHLIP® peptides have medical utility, since they can

target acidic diseased tissues, such as tumors, and deliver therapeutic cargo molecules across membrane or target nanoparticles to cancer cells. Wide medical efficacy of pHLIP® peptides were shown in imaging (16-21) and therapeutic (22-27) applications.

The peptides of pHLIP® family exhibit in three major states: the State I is attributed to the peptides in a coil conformation in aqueous solution at >pH7.4; if a membrane is introduced into the system, the peptides stay in equilibrium between aqueous free and membrane-bound states, which is called the State II. Finally, when pH is lowered (<pH6.0) the Asp/Glu residues in pHLIP® peptides are protonated, which enhances peptide hydrophobicity and promotes peptide partition into bilayer, which is accompanied by folding. The system reaches minimum of free energy, when peptides adopt TM helical conformation, which is assigned to the State III. Thermodynamics and kinetics studies were carried to establish molecular mechanism of peptide's adsorption by the bilayer (transition from State I to State II) and insertion into the membrane (transition from State II to State III) (10, 12, 28, 29). Our ultimate goal is to introduce physical model, which describes spontaneous insertion of a polypeptide into anisotropic environment of lipid bilayer and formation of a polypeptide helical structure. We already did first step, and proposed mathematical formalism describing coil-helix transition of a polypeptide adsorbed at the membrane (30). In order to introduce thermodynamics and kinetics models we have to get full knowledge about both conformational changes within a polypeptide and a membrane during peptide insertion and folding. In all previous studies the main emphasis was on monitoring of conformational changes, which occur in the pHLIP® peptides. Here we used small angle x-ray scattering (SAXS) to monitor changes, which might occur within the lipid bilayer of POPC liposomes, when WT pHLIP® peptide interacts with liposomes at high and low pH values. We selected to work with WT pHLIP® peptide and POPC liposome system, since the system was

very intensively characterized previously and changes in SAXS signal could be attributed to particular events of peptide-membrane interactions.

X-ray and neutron scattering methods have been widely used to elucidate the nanostructure of vesicles and oriented membranes (31-33). These techniques are sensitive to both membrane thickness perturbations and lateral inhomogeneities(31, 34). In the case of unilamellar vesicles, the mean radius, size polydispersity, average membrane thickness and internal membrane structure can be derived by means of the separated form factor model (35, 36). Here we have used SAXS over an extended size scale to monitor changes to the unilamellar vesicle form factor and membrane nanostructure.

Experimental Procedures

Peptides preparation

WT pHLIP® peptide (AEQNPIYWARYADWLFTTPLLLLDLALLVDADEGT) was synthesized and purified at W.M. KECK Biotechnology center at Yale. The synthesized peptide was dissolved directly in buffer and then centrifuged to remove large aggregates. Concentration of the peptide was calculated spectrophotometrically by measuring absorbance at 280 nm using extinction coefficient $\varepsilon_{280} = 13{,}940\ M^{-1}\ cm^{-1}$.

Liposomes preparation

Large unilamellar and multilamellar vesicles were prepared by extrusion. POPC, 1-palmitoyl-2-oleoyl-sn-glycero-3-phosphocholine (Avanti Polar Lipids) was dissolved in chloroform, desolvated in a rotary evaporator and dried under high vacuum for several hours. The phospholipid film was then rehydrated in 10 mM phosphate buffer pH 8.0, vortexed until the

lipid bilayer was completely dissolved, and extruded 51 times through the membranes with 50 nm pore sizes.

Steady-state fluorescence and CD

Steady-state fluorescence, circular dichroism (CD and OCD) measurements were carried out under a temperature control at 25°C on a PC1 spectrofluorometer (ISS, Inc.) and MOS 450 spectropolarimeter (Bio-Logic, Inc.), respectively. The concentration of the peptide and POPC lipids was 150 μM and 4.4 mM, respectively. Tryptophan fluorescence of the peptide was excited at 295 nm and recorded with the excitation and emission slits set at 1 nm. The polarizers in the excitation and emission paths were set at the "magic" angle (54.7^o from the vertical orientation) and vertically (0^o), respectively. Peptide CD spectra were recorded from 190 to 260 nm (where no PMT saturation was observed) with 0.5 nm increment using a cuvette with an optical path length of 0.5 cm.

Small Angle X-ray Scattering (SAXS)

Synchrotron SAXS measurements were carried out at beamline ID02 of the ESRF in Grenoble, France (33). The incident x-ray wavelength (λ) was 0.995 Å and the sample-to-detector distances were 3 m and 1 m, covering a scattering vector range of 0.03 – 6 nm^{-1}. The magnitude of the scattering vector, q, is defined as $q=(4\pi/\lambda)\sin(\theta/2)$, with θ the scattering angle. Samples were contained in a temperature controlled (25°C) flow through quartz capillary cell with a diameter of 1.8 mm. The measured two dimensional SAXS patterns were normalized to an absolute intensity scale using the standard procedure and azimuthally averaged to obtain the intensity profile as a function of q (33). Typical exposure time was 0.1 sec (with an incident flux of 10^{13}

photons/sec) and 3-4 frames were acquired for each sample, which were subsequently averaged after excluding any possible radiation damage. The background buffer was also measured by the same procedure with 10 frames in each case. The averaged buffer background was subtracted from each averaged sample intensity profile to obtain the presented *I(q)* data. In different experiments, the concentration of the peptide was 150 or 300 μM, and POPC liposomes of nominal size of 50 nm was 4.4 or 8.8 mM. SAXS intensities were measured for original POPC liposomes and those incubated with peptide at pH 8.0 and 5.0, as well as peptide alone in buffer. In addition, we carried out measurements with 100 nm and 200 nm liposomes: the overall trend was the same, however their analysis is more complicated due to the presence of multilamellar structure.

Analysis of SAXS data

The background subtracted scattered intensity from a suspension of particulate system can be expressed as,

$$I(q) = N\ F(q)^2 S(q) \qquad (1)$$

where N is the number of particles per unit volume, $F(q)^2$ is the single particle scattering function whose amplitude is given by the Fourier transform of the radial electron density profile and $S(q)$ is the structure factor describing the interaction between particles. In this study, the suspensions are relatively dilute (volume fraction less than 0.01) and the interaction between particles can be neglected corresponding to $S(q)\approx 1$. In the case of WT peptide in solution, $F(q)^2$ is described by a geometric shape (cylinder) with a homogeneous scattering contrast (33). For unilamellar vesicles, the radius R, polydispersity and the membrane internal structure can be simultaneously evaluated using the separated form factor model (31-33, 35, 36). The scattering

contrast is essentially coming from the bilayer region, within the separated form factor model, *F(q,R)* is described by,

$$F(q,R) = 4\pi r_e \int_{-t/2}^{t/2} [\rho(r) - \rho_m] \frac{\sin[(R+r)q]}{(R+r)q} (R+r) dr \quad (2)$$

Where *t* is the bilayer thickness with the origin at the midplane (*r*=0), $\rho(r)$ is the radial electron density of the membrane and ρ_m that of the solvent, and r_e is the classical electron radius. By this definition, *R* is the distance from the center of the vesicle to the midplane of the bilayer. The $\rho(r)$ of phospholipid membrane is approximately described by three Gaussian functions corresponding to the head group regions on both sides and middle hydrophobic chains. (33, 36)

$$\rho(r) = \sum_{i=1}^{3} \rho_i \cdot exp\left[-\frac{(r-R_i)^2}{2\sigma_i^2}\right] \quad (3)$$

Where $\rho_1 = \rho_3$ and ρ_2 are the electron densities of the lipid head group and chain regions, respectively, R_i is the distance from the center of the group to the bilayer midplane, and σ_i is the width of the corresponding Gaussian function. The excess electron densities of head group and the hydrophobic chains from the buffer, $\rho_1-\rho_m$ and $\rho_2-\rho_m$, are denoted by $\Delta\rho_H$, and $\Delta\rho_C$, respectively. Corresponding widths of the Gaussian function are represented by D_H and D_C, and the distance from the midplane of the bilayer to the center of head group as X_H (33, 36).

F(q,R) is given by the separated form factor within the thin shell assumption (35, 36). However, real vesicles have a finite size distribution and Eq. (1) needs to be weighted over the size distribution, *f(R)*, which in this case is assumed to be Schulz size distribution (33, 36). In addition, $S(q) \approx 1$ since the volume fraction of unilamellar vesicles is of the order of 0.01 and POPC is not charged.

$$I(q) = N \int_0^\infty F(q,R)^2 \ f(R) dR \quad (4)$$

Model fits using Eq. (4) yields the mean radius (R_V) and polydispersity (p_V) of the unilamellar vesicles, size of the head group and tail regions and the corresponding electron densities. It is assumed that the same geometric shape of the vesicle is maintained but the height and widths of the three Gaussian functions in Eq. (3) change when peptide interacts with lipid bilayer of membrane.

Results

We employed SAXS to follow changes in the lipid bilayer of POPC liposomes induced by WT pHLIP® peptide adsorption at pH 8.0 and insertion at pH 5.0. These experiments were carried out at much higher peptide and lipid concentrations (150 μM and 300 μM for peptides and 4.4 mM and 8.8 mM for POPC lipids) as compared to concentrations of peptides and lipids used before in biophysical studies. Previously we have shown that WT pHLIP® peptide is monomeric in aqueous solution at pH 8.0 at concentration of 7 μM and less, however it oligomerizes and forms tetramers at concentration of 50 μM (37). Here we first measured CD, fluorescence and scattering profile of 150 and 300 μM of WT peptide at pH 8.0. The position of maximum of fluorescence spectrum of WT peptide is 341 nm (Figure 1), and is very similar to the values established previously for 50 μM of the peptide (37). CD spectrum shows negative signal at 232 nm (Figure 2) characteristic of exciton formation. Exciton (sharing of electronic density) is observed, when rings of several aromatic residues form stacks (38). The exciton formation was monitored previously for 50 μM of the peptide (37). At the same time, we do not observe appearance of any elements of secondary structure for WT peptide at 150 μM at pH 8.0.

SAXS measurements provided very similar results for 150 and 300 μM of WT pHLIP® peptide at pH 8.0. Figure 3 shows the scattering of 300 μM of WT pHLIP® peptide in solution of pH 8.0

and pH 5.0. The scattering curves can be described well by Eq. (1) with $F(q)^2$ the scattering function of polydisperse cylinders (33) and $S(q) \approx 1$. Although a solid cylinder or disk may not be the exact geometrical form the peptide oligomers adopt in solution, the model serves to indicate the approximate lateral dimensions and association states. The fit parameters including an additive constant background (I_B) are summarized in Table 1.

We employed the cylindrical model to find the mean radius (R_C) and the height (H_C) of the cylinder describing scattering profile of WT pHLIP® peptide in solution at pH 8.0 is about 1.37 nm and 6.4 nm, respectively, which corresponds to the cylinder volume of about 38 nm^3. If we assume coil configuration (which is supported by CD data) of $\boldsymbol{N}$ = 35 residues long WT pHLIP® peptide and take into account that the contour length per residue (established previously) $\boldsymbol{L}$ = 4.3 Å or 0.43 nm (39-41), then the average end-to-end length of the coil can be estimated to be $\boldsymbol{d} = \boldsymbol{L}\sqrt{\boldsymbol{N}}$ = 2.5 nm. Then for spherical shape, the volume occupied by a single WT peptide in a random coil conformation is about 8.2 nm^3. Thus, about 4 peptides in a random coil configuration can occupy volume of about 33-44 nm^3 depending on the packing parameter. It is an interesting and important finding that WT pHLIP® peptide transfers from its monomeric form at <10 μM at pH 8.0 to tetrameric oligomer at 50 μM and remains in the terameric form at high concentrations (at least up to 300 μM). At lower pH, WT pHLIP® peptide formed much bigger aggregates which can also be approximately described by a cylinder scattering function but with very different aspect ratio. The model curve for pH 4 in Figure 3 corresponds to a mean radius of 14 nm with 10% polydispersity and height of 5.4 nm. These parameters suggest that the pHLIP® chains have further coiled and aggregated laterally to form a flat disk-like object at low pH.

Next, we proceed to experiments on liposomes. Since spectral signals (especially CD) are destroyed by scattering from high concentration of liposomes (more than 4 mM of lipids), we

prepared samples of 150 μM WT pHLIP® peptide in State I (peptide at pH 8.0, no liposomes), State II (peptide at pH 8.0 and 4 mM POPC liposomes) and State III (peptide at pH 5.0 with 4 mM POPC liposomes). Then, each sample was diluted 7 times and CD and fluorescence spectra were measured immediately. The changes of fluorescence signal (Figure 4) is typical for pHLIP® peptides (12, 19, 37) resulting in increase of fluorescence intensity and shift of the position of maximum of emission to shorter wavelengths, which is indicative of pH-dependent insertion into the lipid bilayer of membrane. CD demonstrates presence of exciton structures in the State I indicative of oligomerization (Figure 5). Also, the exciton signal was observed for the peptide in the presence of membrane at pH 8.0. We need to outline that at low lipid:peptide ratio (it is 27 in our case) we expect to have significant population of membrane unbound peptides, since at pH 8.0 one peptide interacts with about 50 lipid head groups on average (28). At the same time, at low pH, the affinity of the peptide to membrane is higher and one peptide interacts with about 10-15 lipids on average (28). As a result, the main population of peptides is in a membrane-inserted, helical conformation, which is supported by the CD spectrum with minimum at 225 nm.

In Figure 6, we present the SAXS from POPC vesicles in the absence and presence of WT pHLIP® peptide. Because of the cancelling effect of positive and negative contrasts from the lipid head group and hydrophobic chains, respectively, the net low q forward scattering from pure POPC vesicles is rather weak and barely measurable over the buffer and instrument background. The main feature in SAXS is the bilayer form factor, which can be described by Eq. (4) confirming the unilamellar nature of the liposomes with mean radius about 28.5 nm. There is no significant variation in the bilayer form factor with pH and shape of the curves. The best fit excess electron density profiles using Eqs. (3) and (4) are displayed in Figure 7. As expected, the membrane electron density profiles of pure POPC liposomes perfectly superimpose

at higher and lower pH values. The same scattering features are observed at lower POPC concentrations with factor 2 and 4 dilutions but the intensity statistics at high q values become poorer. The obtained electron density profile of POPC unilamellar liposomes is comparable to that reported for oriented lipid membranes (32, 42) though less structured [for a similar model as in Eq. (3)] presumably due to shape fluctuations.

With the addition of WT pHLIP® peptide, the low q scattering features of POPC vesicles became more pronounced as a result of an increase in the positive contrast of the phospholipid membrane. Indeed, these low q scattering features are different from the pure peptide scattering profiles presented in Figure 3. At pH 8.0 a fraction of the peptides remained free in the solution. In Equation (4), it was necessary to include either a constant background or a fraction of free peptide (up to 30%) intensity to obtain a complete description of the data. However, at low pH in presence of membrane, larger peptide aggregates as that depicted in Figure 3 could not be observed, since most of the peptides were inserted into the membrane. The SAXS data are in agreement with CD measurements. Main parameters of the SAXS model are tabulated in Table 2.

At low pH, typical unilamellar liposome scattering signature became more evident confirming that WT pHLIP® peptide has inserted into the membrane thereby significantly enhancing the positive contrast of the membranes. Scattering curves with peptide were analyzed using the same parameters of the unilamellar liposomes but the membrane electron density profile was allowed to vary. The corresponding excess electron density profiles are shown in Figure 7. At higher pH (pH 8.0), the inner hydrophibic part has similar shape as the pure POPC liposomes indicating the peptide molecules were residing at the outer leaflets of the membranes. This has led to an increase in the electron density of the head group region without significant broadening of the

peak implying that peptide chains have penetrated into the head group region. However, at lower pH (pH 5.0) both the inner and outer electron densities have increased meaning that the peptides have been inserted across the bilayer of the membrane. In addition, the peak at the outer hydrophilic part has significantly broadened implying that both ends of the peptide imposing steric constraints on the lipid head groups. The resulting enhanced electron density led to stronger low q scattering feature of the unilamellar liposomes.

Discussion

The pHLIP® peptides find wide application in biomedical sciences (16, 21, 22, 43, 44) and, also, they prove to be very convenient model system for the investigation of a polypeptide insertion into lipid bilayer of membrane triggered by pH (12, 28, 30). While various spectroscopic methods employed previously probed changes to the conformation of peptide, SAXS employed in this study allowed us, for the first time, to monitor the changes to the liposome and lipid bilayer structure. Until now, most experiments were carried out at low peptide concentration (about 2 – 10 μM) and high lipid:peptide ratios (about 100 – 300). In this study we used high peptide concentration (about 150 – 300 μM) and low lipid:peptide ratio (about 30). First we investigated WT pHLIP® peptide conformational states in solution in absence of liposomes at high and low pH. Interestingly that at the range of concentrations from 50 μM up to 300 μM peptides remained in tetrameric configuration and does not form larger aggregates at pH 8. It is a very important finding related to potential medical applications, when high dosage of pHLIP® peptides could be required for human administration. At low pH, when Asp and Glu residues are protonated, peptide in solution in absence of liposomes forms higher order of aggregates. However, in the presence of membrane these larger aggregates were not observed at

low pH. The interaction of WT pHLIP® peptide with liposomes has not altered the unilamellar vesicle structure upon peptide adsorption by lipid bilayer at high pH or upon insertion across the bilayer at low pH. From the analysis of SAXS data, an average change in the electron density profile of the membrane upon insertion of WT pHLIP® peptide was derived. It is clearly shown the insertion of the peptide into the membrane at lower pH corresponding to a significant increase in the electron density and low q scattering. The membrane electron density profiles of POPC unilamellar vesicles without peptides are comparable to those reported in the literature for oriented POPC membranes (32, 42). Although, the model could be improved further with additional Gaussian terms in Eq. (3), it was sufficient to capture the main structural features of the POPC-WT pHLIP® liposomes.

Figure 8 schematically illustrates the behavior of the peptide in aqueous solution at low and high concentrations, and interactions with membrane at low and high pH values derived from numerous previous and current spectroscopic and SAXS studies. At high/neutral pH and at low concentration (< 7 μM), the peptide is monomeric in aqueous solution (37). With increase of peptide concentration (up to 30 μM), WT pHLIP® peptide is associated into tetrameric oligomers and stays as a tetramer with concentration increase by about 10 fold (and potentially even higher concentrations). When excess of membrane is present, the equilibrium is shifted towards membrane-adsorbed state of the peptide (called state II). Depending on lipid:peptide ratio, polypeptide can adopt different conformations within a membrane. At low lipid:peptide ratios the "parking problem" exists, which results in partial adsorption of WT pHLIP® peptide by membrane, oppose to the extended peptide configuration at the surface of lipid bilayer at high lipid:peptide ratios (28). Also depending on hydrophobicity of the polypeptide sequence and presence of charged residues, various pHLIP® peptides exhibit different penetration depths

within the bilayer (10, 45). Our data, obtained in this study, indicate that WT pHLIP® peptide is adsorbed within the polar headgroup region of the bilayer. Drop of pH results in protonation of Asp/Glu residues, increase of overall polypeptide hydrophobicity, which triggers polypeptide partitioning into membrane and folding. Most of pHLIP® peptides adopt very similar transmembrane helical orientation (called state III)(10). We have shown that at low peptide concentration transmembrane helices do not oligomerize (37). Our scattering data obtained on liposomes with WT pHLIP® peptide at low pH suggest uniform distribution of helices at high peptide concentration and low lipid:peptide ratios. However, further investigation is required to address this question.

The obtained results clearly indicate that SAXS could be used to monitor polypeptide interactions with lipid bilayer of membrane in real time upon pH change. Our next step will be a kinetic study directed toward monitoring changes of SAXS intensities upon peptide insertion into membrane and exit from the membrane with pH jumps in correlation with changes of tryptophan fluorescence signal of the peptide.

TABLES

Table 1. Analysis of SAXS data obtained from 300 μM solutions of WT pHLIP® peptide in PBS buffer at pH 8.0 and pH 5.0. Normalized SAXS intensities can be described by a polydisperse cylinder scattering function with parameters, mean radius (R_C), height (H_C), polydispersity in radius (p_C), and a constant background (I_B).

pH	R_C (nm)	H_C (nm)	p_C	I_B (mm^{-1})
8.0	1.37	6.4	0.1	$4x10^{-5}$
5.0	14.0	5.4	0.1	$1x10^{-4}$

Table 2: Main parameters derived from SAXS modeling of data in Figure 6 by means of the separated form factor approach. Parameters R_V, p_V, $\Delta\rho_H$, $\Delta\rho_C$, D_H, D_C, X_H, and I_B represent mean vesicle radius, vesicle size polydispersity, excess electron densities of head group and hydrophobic chains, Gaussian widths of the head group and hydrophobic chains, distance to center of the head group from the bilayer midplane, and a constant background, respectively.

Sample	R_V (nm)	p_V	$\Delta\rho_H$ (nm^{-3})	$\Delta\rho_C$ (nm^{-3})	D_H (nm)	D_C (nm)	X_H (nm)	I_B (mm^{-1})
POPC-8.8mM pH 8.0	28.0	0.28	23.1	-23.2	0.36	0.66	1.8	$7x10^{-5}$
POPC-8.8mM pH 5.0	28.0	0.28	22.5	-23.2	0.36	0.65	1.8	$8x10^{-5}$
POPC-4.4mM WT-150μm pH 8.0	28.6	0.30	26.3	-23.2	0.33	0.67	1.82	$5x10^{-5}$
POPC-4.4mM WT 150μm pH 5.0	28.3	0.23	28.1	-20.7	0.48	0.94	1.8	$8x10^{-5}$

FIGURES

Figure 1. Tryptophan fluorescence excited at 295 nm of 150 μM of WT pHLIP® peptide in phosphate buffer at pH 8.0.

Figure 2. Circular dichroism signal of 150 μM of WT pHLIP® peptide in phosphate buffer at pH 8.0.

Figure 3. Normalized SAXS intensities obtained from 300 μM solutions of WT pHLIP® peptide at pH 8.0 and pH 5.0. At pH 8.0, the scattering profile is described by a cylinder-like function corresponding to a tetrameric form of the peptide. At pH 5.0 in the absence of membrane, WT pHLIP® peptide forms large flat aggregates. Table 1 summarizes the results of data analysis.

Figure 4. Three states of WT pHLIP® peptide were monitored by changes of tryptophan fluorescence. The state I (black line) represents peptide in solution at pH 8.0. The state II (blue line) is a peptide in a solution in the presence of POPC liposomes at pH 8.0. The state III (red line) is a peptide in a solution in the presence of POPC liposomes at pH 5.0.

Figure 5. Three states of WT pHLIP® peptide were monitored by changes of CD signal. The state I (black line) represents peptide in solution at pH 8.0. The state II (blue line) is a peptide in a solution in the presence of POPC liposomes at pH 8.0. The state III (red line) is a peptide in a solution in the presence of POPC liposomes at pH 5.0.

Figure 6. SAXS intensities from the POPC liposomes of nominal diameter 50 nm without and with WT pHLIP® peptide. The low q region shows the unilamellar vesicle features while the high q region depicts the prototypical bilayer form factor. Data were analyzed using polydisperse unilamellar model with three Gaussian electron density profiles for the lipid bilayer using

Equations (3) and (4). Main parameters of the model are tabulated in Table 2. For clarity successive scattering curves have been multiplied by the factors indicated in parenthesis.

Figure 7. Excess electron density profiles (above buffer level) presented as a sum of three Gaussian functions obtained from the analysis of SAXS intensities presented in Figure 6.

Figure 8. Schematic presentation of WT pHLIP® peptide interaction with lipid bilayer of membrane, see description in the text.

AUTHOR INFORMATION

Corresponding Authors

* Theyencheri Narayanan, ESRF, CS40220, 38043 Grenoble, France; Phone: +33 4 76 88 21 21; E-mail: narayan@esrf.fr.

Present Addresses

†Department of Molecular Biophysics and Biochemistry, Yale University, New Haven, CT 06520.

Author Contributions

T.N., O.A.A. and Y.K.R. design research; D.W., A.G.K., M.A. and T.N. performed SAXS measurements and D.W. performed spectral measurements; T.N. analyzed SAXS data; D.W., O.A.A., Y.K.R. and T.N. wrote paper.

Abbreviations

CD, circular dichroism; ED, electron density; PBS – phosphate buffer saline; pHLIP, pH Low Insertion Peptide; POPC, 1-palmitoyl-2-oleoyl-sn-glycero-3-phosphocholine; SAXS, small angle x-ray scattering; TM, transmembrane; WT, wild type.

Acknowledgment

This work was supported by the National Institute of Health grant number GM073857 to OAA and YKR. ESRF is acknowledged for synchrotron beam time.

REFERENCES

1. Van den Berg, B., Clemons, W.M., Jr., Collinson, I., Modis, Y., Hartmann, E., Harrison, S.C.Rapoport, T.A. X-ray structure of a protein-conducting channel. *Nature* **2004**, 427, 36-44, DOI: 10.1038/nature02218.
2. Osborne, A.R., Rapoport, T.A.van den Berg, B. Protein translocation by the Sec61/SecY channel. *Annu Rev Cell Dev Biol* **2005**, 21, 529-550, DOI: 10.1146/annurev.cellbio.21.012704.133214.
3. White, S.H.von Heijne, G. The machinery of membrane protein assembly. *Curr Opin Struct Biol* **2004**, 14, 397-404, DOI: 10.1016/j.sbi.2004.07.003.
4. Simpson, P.J., Schwappach, B., Dohlman, H.G.Isaacson, R.L. Structures of Get3, Get4, and Get5 provide new models for TA membrane protein targeting. *Structure* **2010**, 18, 897-902, DOI: 10.1016/j.str.2010.07.003.
5. Brambillasca, S., Yabal, M., Makarow, M.Borgese, N. Unassisted translocation of large polypeptide domains across phospholipid bilayers. *J Cell Biol* **2006**, 175, 767-777, DOI: 10.1083/jcb.200608101.
6. Renthal, R. Helix insertion into bilayers and the evolution of membrane proteins. *Cellular and molecular life sciences : CMLS* **2010**, 67, 1077-1088, DOI: 10.1007/s00018-009-0234-9.
7. Ladokhin, A.S.White, S.H. Interfacial folding and membrane insertion of a designed helical peptide. *Biochemistry* **2004**, 43, 5782-5791, DOI: 10.1021/bi0361259.
8. Hunt, J.F., Earnest, T.N., Bousche, O., Kalghatgi, K., Reilly, K., Horvath, C., Rothschild, K.J.Engelman, D.M. A biophysical study of integral membrane protein folding. *Biochemistry* **1997**, 36, 15156-15176, DOI: 10.1021/bi970146j.

9. Reshetnyak, Y.K., Andreev, O.A., Lehnert, U.Engelman, D.M. Translocation of molecules into cells by pH-dependent insertion of a transmembrane helix. *Proc Natl Acad Sci U S A* **2006**, 103, 6460-6465, DOI: 0601463103.

10. Weerakkody, D., Moshnikova, A., Thakur, M.S., Moshnikova, V., Daniels, J., Engelman, D.M., Andreev, O.A.Reshetnyak, Y.K. Family of pH (low) insertion peptides for tumor targeting. *Proc Natl Acad Sci U S A* **2013**, 110, 5834-5839, DOI: 10.1073/pnas.1303708110.

11. Musial-Siwek, M., Karabadzhak, A., Andreev, O.A., Reshetnyak, Y.K.Engelman, D.M. Tuning the insertion properties of pHLIP. *Biochim Biophys Acta* **2010**, 1798, 1041-1046, DOI: S0005-2736(09)00309-5.

12. Karabadzhak, A.G., Weerakkody, D., Wijesinghe, D., Thakur, M.S., Engelman, D.M., Andreev, O.A., Markin, V.S.Reshetnyak, Y.K. Modulation of the pHLIP transmembrane helix insertion pathway. *Biophys J* **2012**, 102, 1846-1855, DOI: 10.1016/j.bpj.2012.03.02.

13. Barrera, F.N., Weerakkody, D., Anderson, M., Andreev, O.A., Reshetnyak, Y.K.Engelman, D.M. Roles of carboxyl groups in the transmembrane insertion of peptides. *J Mol Biol* **2011**, 413, 359-371, DOI: S0022-2836(11)00877-1.

14. Onyango, J.O., Chung, M.S., Eng, C.H., Klees, L.M., Langenbacher, R., Yao, L.An, M. Noncanonical amino acids to improve the pH response of pHLIP insertion at tumor acidity. *Angew Chem Int Ed Engl* **2015**, 54, 3658-3663, DOI: 10.1002/anie.201409770.

15. Nguyen, V.P., Alves, D.S., Scott, H.L., Davis, F.L.Barrera, F.N. A Novel Soluble Peptide with pH-Responsive Membrane Insertion. *Biochemistry* **2015**, 54, 6567-6575, DOI: 10.1021/acs.biochem.5b00856.

16. Tapmeier, T.T., Moshnikova, A., Beech, J., Allen, D., Kinchesh, P., Smart, S., Harris, A., McIntyre, A., Engelman, D.M., Andreev, O.A., et al. The pH low insertion peptide pHLIP Variant 3 as a novel marker of acidic malignant lesions. *Proc Natl Acad Sci U S A* **2015**, 112, 9710-9715, DOI: 10.1073/pnas.1509488112.

17. Viola-Villegas, N.T., Carlin, S.D., Ackerstaff, E., Sevak, K.K., Divilov, V., Serganova, I., Kruchevsky, N., Anderson, M., Blasberg, R.G., Andreev, O.A., et al. Understanding the pharmacological properties of a metabolic PET tracer in prostate cancer. *Proc Natl Acad Sci U S A* **2014**, 111, 7254-7259, DOI: 10.1073/pnas.1405240111.

18. Cruz-Monserrate, Z., Roland, C.L., Deng, D., Arumugam, T., Moshnikova, A., Andreev, O.A., Reshetnyak, Y.K.Logsdon, C.D. Targeting pancreatic ductal adenocarcinoma acidic microenvironment. *Sci Rep* **2014**, 4, 4410, DOI: 10.1038/srep04410.

19. Sosunov, E.A., Anyukhovsky, E.P., Sosunov, A.A., Moshnikova, A., Wijesinghe, D., Engelman, D.M., Reshetnyak, Y.K.Andreev, O.A. pH (low) insertion peptide (pHLIP) targets ischemic myocardium. *Proc Natl Acad Sci U S A* **2013**, 110, 82-86, DOI: 10.1073/pnas.1220038110.

20. Daumar, P., Wanger-Baumann, C.A., Pillarsetty, N., Fabrizio, L., Carlin, S.D., Andreev, O.A., Reshetnyak, Y.K.Lewis, J.S. Efficient (18)F-labeling of large 37-amino-acid pHLIP peptide analogues and their biological evaluation. *Bioconjug Chem* **2012**, 23, 1557-1566, DOI: 10.1021/bc3000222.

21. Reshetnyak, Y.K., Yao, L., Zheng, S., Kuznetsov, S., Engelman, D.M.Andreev, O.A. Measuring tumor aggressiveness and targeting metastatic lesions with fluorescent pHLIP. *Mol Imaging Biol* **2011**, 13, 1146-1156, DOI: 10.1007/s11307-010-0457-z.

22. Antosh, M.P., Wijesinghe, D.D., Shrestha, S., Lanou, R., Huang, Y.H., Hasselbacher, T., Fox, D., Neretti, N., Sun, S., Katenka, N., et al. Enhancement of radiation effect on cancer cells by gold-pHLIP. *Proc Natl Acad Sci U S A* **2015**, 112, 5372-5376, DOI: 10.1073/pnas.1501628112.

23. An, M., Wijesinghe, D., Andreev, O.A., Reshetnyak, Y.K.Engelman, D.M. pH-(low)-insertion-peptide (pHLIP) translocation of membrane impermeable phalloidin toxin inhibits cancer cell proliferation. *Proc Natl Acad Sci U S A* **2010**, 107, 20246-20250, DOI: 1014403107.

24. Moshnikova, A., Moshnikova, V., Andreev, O.A.Reshetnyak, Y.K. Antiproliferative effect of pHLIP-amanitin. *Biochemistry* **2013**, 52, 1171-1178, DOI: 10.1021/bi301647y.

25. Cheng, C.J., Bahal, R., Babar, I.A., Pincus, Z., Barrera, F., Liu, C., Svoronos, A., Braddock, D.T., Glazer, P.M., Engelman, D.M., et al. MicroRNA silencing for cancer therapy targeted to the tumour microenvironment. *Nature* **2014**, DOI: 10.1038/nature13905.

26. Burns, K.E.Thevenin, D. Down-regulation of PAR1 activity with a pHLIP-based allosteric antagonist induces cancer cell death. *Biochem J* **2015**, 472, 287-295, DOI: 10.1042/BJ20150876.

27. Burns, K.E., Robinson, M.K.Thevenin, D. Inhibition of cancer cell proliferation and breast tumor targeting of pHLIP-monomethyl auristatin E conjugates. *Mol Pharm* **2015**, 12, 1250-1258, DOI: 10.1021/mp500779k.

28. Reshetnyak, Y.K., Andreev, O.A., Segala, M., Markin, V.S.Engelman, D.M. Energetics of peptide (pHLIP) binding to and folding across a lipid bilayer membrane. *Proc Natl Acad Sci U S A* **2008**, 105, 15340-15345, DOI: 0804746105.

29. Andreev, O.A., Karabadzhak, A.G., Weerakkody, D., Andreev, G.O., Engelman, D.M.Reshetnyak, Y.K. pH (low) insertion peptide (pHLIP) inserts across a lipid bilayer as a helix and exits by a different path. *Proc Natl Acad Sci U S A* **2010**, 107, 4081-4086, DOI: 10.1073/pnas.0914330107.

30. Sharma, G.P., Reshetnyak, Y.K., Andreev, O.A., Karbach, M.Muller, G. Coil-helix transition of polypeptide at water-lipid interface. *J. Stat. Mech.* **2015**, P01034.

31. Kucˇerka, N., Nieh, M.-P.Katsaras, J. Small-Angle Scattering from Homogenous and Heterogeneous Lipid Bilayers. *Advances in Planar Lipid Bilayers and Liposomes* **2010**, 12, 201-235.

32. Kucˇerka, N., Liu, Y., Chu, N., Petrache, H.I., Tristram-Nagle, S.Nagle, J.F. Structure of fully hydrated fluid phase DMPC and DLPC lipid bilayers using X-ray scattering from oriented multilamellar arrays and from unilamellar vesicles. *Biophys J* **2005**, 88, 2626-2637, DOI: S0006-3495(05)73317-8.

33. Narayanan, T., Gummel, J.Gradzielski, M. Probing the Self-Assembly of Unilamellar Vesicles Using Time-Resolved SAXS. *Advances in Planar Lipid Bilayers and Liposomes* **2014**, 20, 171-196.

34. Marquardt, D., Heberle, F.A., Nickels, J.D., Pabst, G.Katsaras, J. On scattered waves and lipid domains: detecting membrane rafts with X-rays and neutrons. *Soft Matter* **2015**, 11, 9055-9072, DOI: 10.1039/c5sm01807b.

35. Kiselev, M.A., Zemlyanaya, E.V., Aswal, V.K.Neubert, R.H. What can we learn about the lipid vesicle structure from the small-angle neutron scattering experiment? *Eur Biophys J* **2006**, 35, 477-493, DOI: 10.1007/s00249-006-0055-9.

36. Pencer, J., Krueger, S., Adams, C.P.Katsaras, J. Method of separated form factors for polydisperse vesicles. *J Appl. Cryst.* **2006**, 39, 293.

37. Reshetnyak, Y.K., Segala, M., Andreev, O.A.Engelman, D.M. A monomeric membrane peptide that lives in three worlds: in solution, attached to, and inserted across lipid bilayers. *Biophys J* **2007**, 93, 2363-2372, DOI: S0006-3495(07)71491-1.

38. Roy, R.S., Gopi, H.N., Raghothama, S., Gilardi, R.D., Karle, I.L.Balaram, P. Peptide hairpins with strand segments containing alpha- and beta-amino acid residues: cross-strand aromatic interactions of facing Phe residues. *Biopolymers* **2005**, 80, 787-799, DOI: 10.1002/bip.20294.

39. Dietz, H.Rief, M. Protein structure by mechanical triangulation. *Proc Natl Acad Sci U S A* **2006**, 103, 1244-1247, DOI: 10.1073/pnas.0509217103.

40. Carrion-Vazquez, M., Li, H., Lu, H., Marszalek, P.E., Oberhauser, A.F.Fernandez, J.M. The mechanical stability of ubiquitin is linkage dependent. *Nat Struct Biol* **2003**, 10, 738-743, DOI: 10.1038/nsb965.

41. Oesterhelt, F., Oesterhelt, D., Pfeiffer, M., Engel, A., Gaub, H.E.Muller, D.J. Unfolding pathways of individual bacteriorhodopsins. *Science* **2000**, 288, 143-146.

42. Pabst, G., Rappolt, M., Amenitsch, H.Laggner, P. Structural information from multilamellar liposomes at full hydration: Full q-range fitting with high quality x-ray data. *Phys Rev E Stat Nonlin Soft Matter Phys* **2000**, 62, 4000-4009.

43. Adochite, R.C., Moshnikova, A., Golijanin, J., Andreev, O.A., Katenka, N.Reshetnyak, Y.K. Comparative study of tumor targeting and biodistribution of pH (Low) Insertion Peptides (pHLIP® peptides) conjugated with different fluorescent dyes. *Mol Imaging Biol* **2016**, in press.

44. Cheng, C.J., Bahal, R., Babar, I.A., Pincus, Z., Barrera, F., Liu, C., Svoronos, A., Braddock, D.T., Glazer, P.M., Engelman, D.M., et al. MicroRNA silencing for cancer therapy targeted to the tumour microenvironment. *Nature* **2015**, 518, 107-110, DOI: 10.1038/nature13905.

45. Zoonens, M., Reshetnyak, Y.K.Engelman, D.M. Bilayer interactions of pHLIP, a peptide that can deliver drugs and target tumors. *Biophys J* **2008**, 95, 225-235, DOI: S0006-3495(08)70298-4.

FIGURES

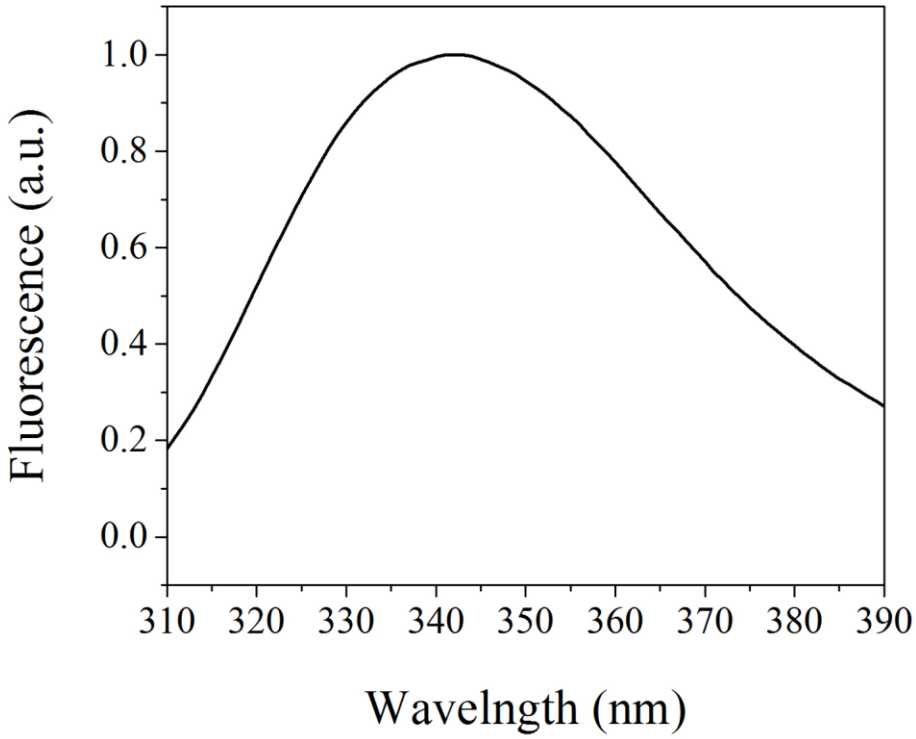

Figure 1

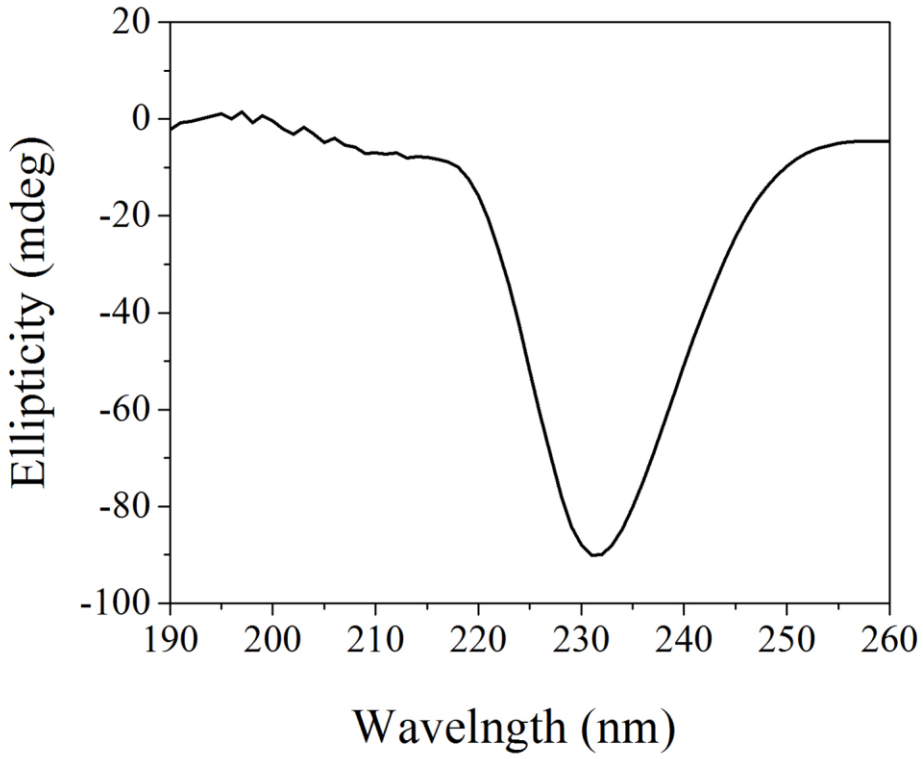
20
0
-20
-40
-60
-80
-100
Ellipticity (mdeg)
190
200
210
220
230
240
250
260
Wavelngth (nm)

Figure 2

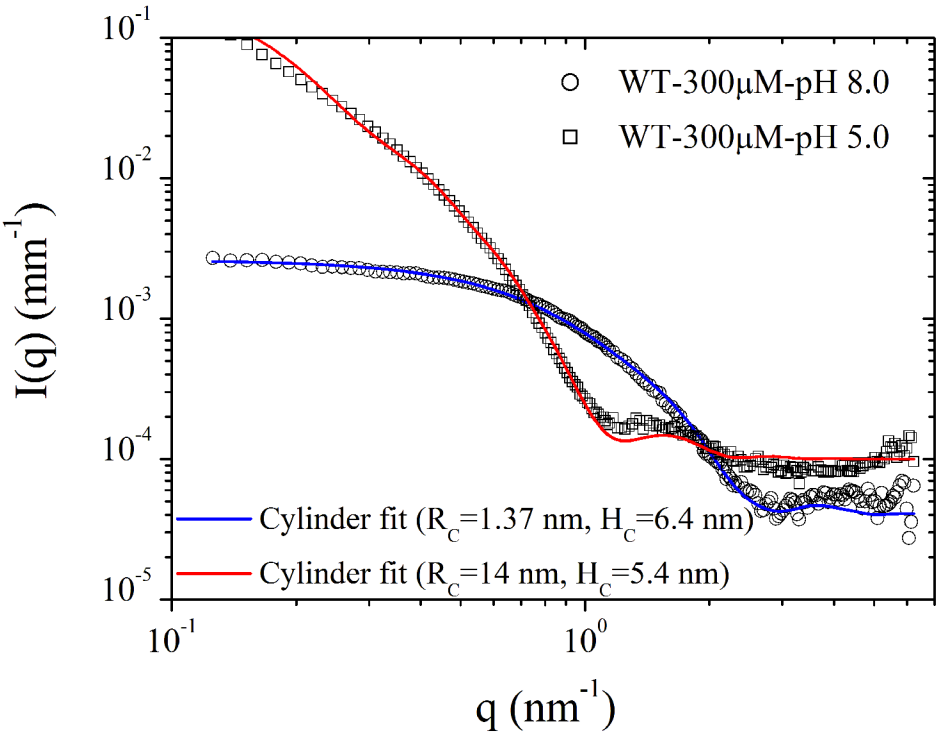
WT-300μM-pH 8.0
WT-300μM-pH 5.0
Cylinder fit (R_C=1.37 nm, H_C=6.4 nm)
Cylinder fit (R_C=14 nm, H_C=5.4 nm)
I(q) (mm^-1)
q (nm^-1)
10^-1
10^-2
10^-3
10^-4
10^-5
10^0

Figure 3

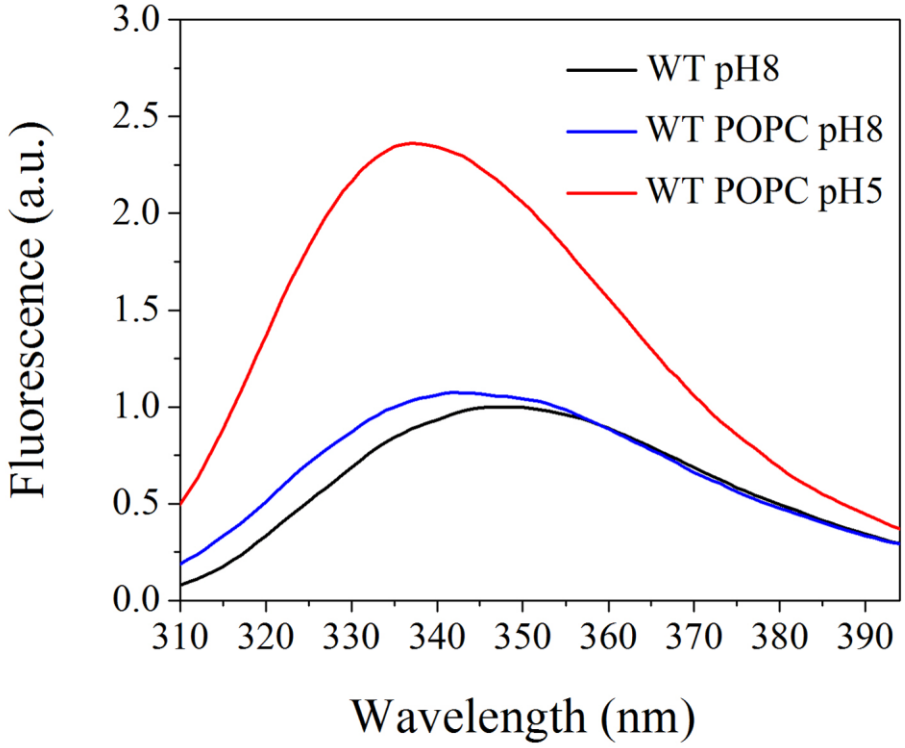
WT pH8
WT POPC pH8
WT POPC pH5
Fluorescence (a.u.)
Wavelength (nm)
3.0
2.5
2.0
1.5
1.0
0.5
0.0
310
320
330
340
350
360
370
380
390

Figure 4

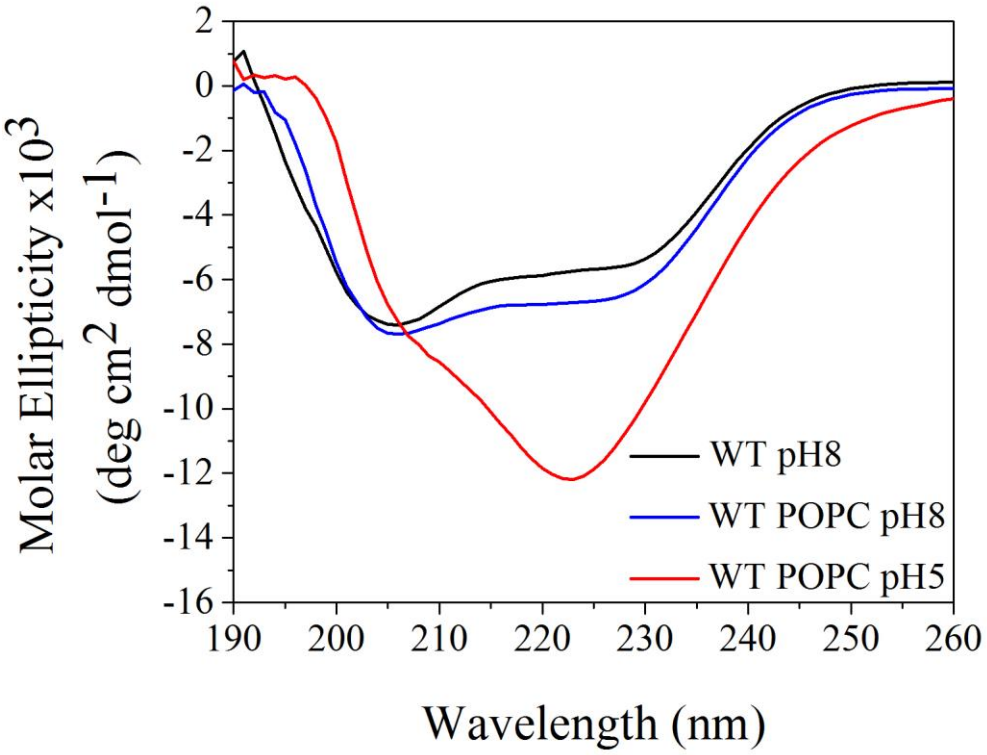
Molar Ellipticity x10^3
(deg cm^2 dmol^-1)
2
0
-2
-4
-6
-8
-10
-12
-14
-16
190
200
210
220
230
240
250
260
Wavelength (nm)
WT pH8
WT POPC pH8
WT POPC pH5

Figure 5

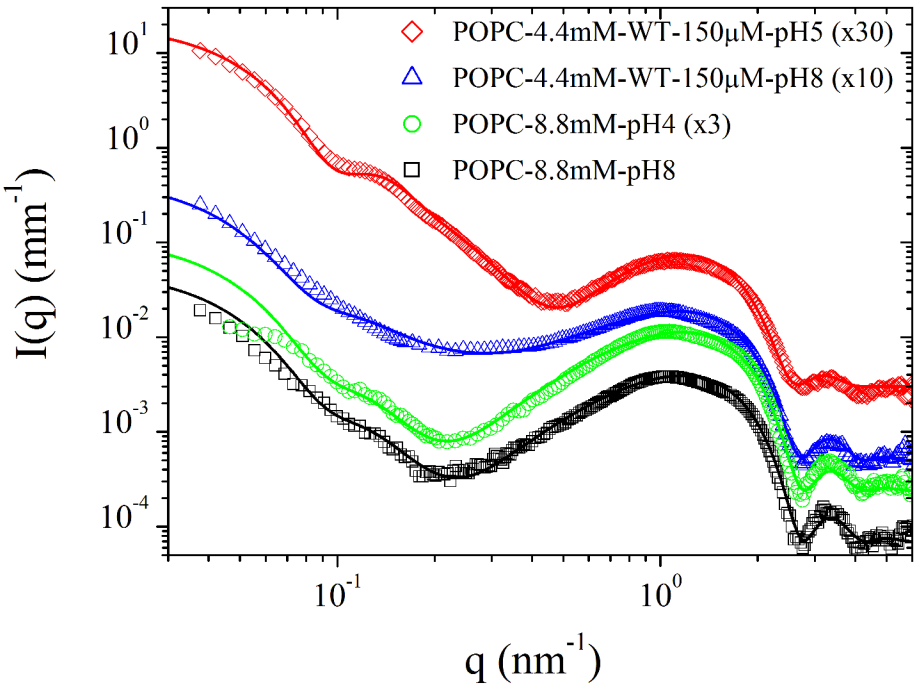
POPC-4.4mM-WT-150μM-pH5 (x30)
POPC-4.4mM-WT-150μM-pH8 (x10)
POPC-8.8mM-pH4 (x3)
POPC-8.8mM-pH8
I(q) (mm-1)
q (nm-1)
10^1
10^0
10^-1
10^-2
10^-3
10^-4
10^-1
10^0

Figure 6

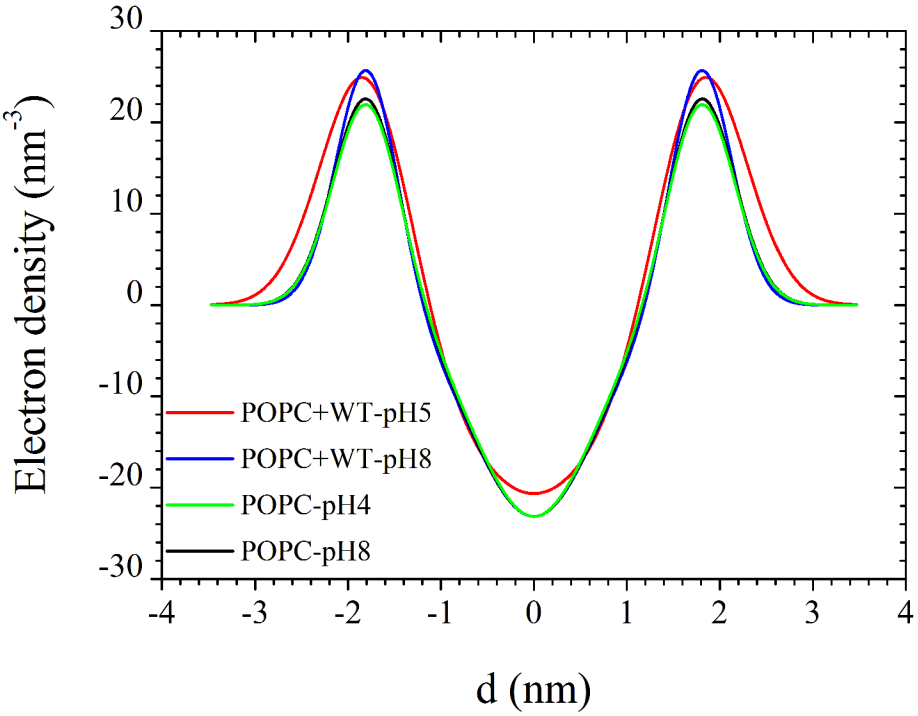
Electron density (nm-3)
d (nm)
POPC+WT-pH5
POPC+WT-pH8
POPC-pH4
POPC-pH8
30
20
10
0
-10
-20
-30
-4
-3
-2
-1
0
1
2
3
4

Figure 7

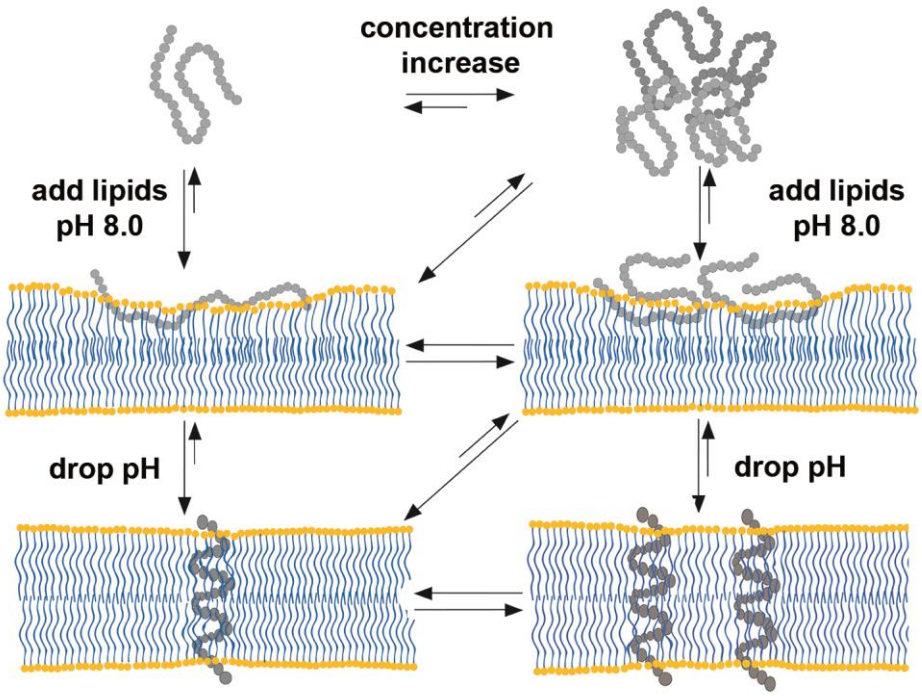
concentration
increase
add lipids
pH 8.0
add lipids
pH 8.0
drop pH
drop pH

Figure 8